WPS1-PR(18) 21497

R. Sharma et al.

2D poloidal profiles and influence of positive and negative density gradients on plasma fluctuations using the Heavy Ion Beam Probe system in the TJ-II stellarator

Preprint of Paper to be submitted for publication in
Nuclear Fusion

This work has been carried out within the framework of the EUROfusion Consortium and has received funding from the Euratom research and training programme 2014-2018 under grant agreement No 633053. The views and opinions expressed herein do not necessarily reflect those of the European Commission.

2D poloidal profiles and influence of positive and negative density gradients on plasma fluctuations using the Heavy Ion Beam Probe system in the TJ-II stellarator

R. Sharma[1a], P.O. Khabanov[2,5], A.V. Melnikov[2,4], C. Hidalgo[1], A. Cappa[1], A. Chmyga[3], G.N. Deshko[3], L.G. Eliseev[2], T. Estrada[1], N.K. Kharchev[2], S.M. Khrebtov[3], A.D. Komarov[3], A.S. Kozachek[3], L.I. Krupnik[3], A. Malaquias[1a], B van Milligen[1], A. Molinero[1], J.L. de Pablos[1], I. Pastor[1], V.N. Zenin[3,5] and the TJ-II team

[1a]*IPFN, Instituto Superior Técnico, Universidade de Lisboa, 1049-001 Lisboa, Portugal*
[1]*Fusion National Laboratory, CIEMAT, 28040, Madrid, Spain*
[2]*National Research Centre 'Kurchatov Institute', 123182, Moscow, Russia*
[3]*Institute of Plasma Physics, NSC KIPT, 611108, Kharkov, Ukraine*
[4]*National Research Nuclear University MEPhI, 115409, Moscow, Russia*
[5]*Moscow Institute of Physics and Technology, 141700, Dolgoprudny, Russia*

Abstract

2D poloidal contour plots of plasma potential and density and their fluctuations have been measured in low density plasmas with hollow density profiles sustained by ECRH in the TJ-II stellarator. The 2D map for the absolute plasma potential shows a local maximum in the plasma core as expected in electron root scenarios and a mismatch with vacuum magnetic calculations that could be partially explained by instrumental effects. Density fluctuations appear both at positive and negative density gradient regions, with normalized level of density fluctuations higher in the negative density gradient region. The TJ-II innovative experimental set-up developed using a dual HIBP diagnostic pave the way for model validation on core plasma potential asymmetries and particle transport under positive density gradient scenarios in the TJ-II stellarator.

I. Introduction

Understanding and predicting particle and energy transport driven by turbulence is a key research issue in magnetically fusion plasmas. Upcoming fusion devices, like ITER, will explore plasma regimes that are far from present devices in many aspects. Therefore, extrapolations from pure empirical data can be misleading and reliable data are required to validate models in existing plasma scenarios.

The characterization of asymmetries in plasma fluctuations is an important topic to understand and validate transport mechanisms in magnetically confined fusion plasma. The search for asymmetries in edge plasma fluctuations has shown the importance of the curvature driven instabilities in the plasma boundary region [1]. First direct experimental evidence of strong poloidal Reynold stress asymmetry [2] also pointed out the curvature driven zonal flow, which is similar to the asymmetry observed in turbulent transport. In addition, flux-surface variations of electrostatic potential can have a significant impact on high-Z impurities radial fluxes [2]. Recent gyrokinetic simulations

in stellarators show a strong localization of unstable modes along the flux surface [3, 4]. 2D core and edge density fluctuations have been previously investigated using beam emission spectroscopy [5] and fast cameras respectively [6]. 2D spatial potential profiles have been measured by heavy ion beam probe in LHD [7].

Another important factor contributing to the particle transport is the density gradient localization, which is closely connected to the refuelling for next step tokamaks and stellarators devices. Fuelling of core plasma particles is foreseen by pellet systems that injects particles at high speed deep into the plasma. However, at reactor relevant plasma densities and temperatures, pellets are unable to reach the core plasma region. In fact, pellet ablation will take place in the plasma edge region [8, 9, 10], causing plasma bumps with positive and negative density gradient regions where eventually particles could be transported radially inwards by turbulence. Fluid and GK simulations have investigated the level of inward turbulent particle transport in the inverted density gradient region [11, 12, 13], but comparisons of simulations with experimental fluctuation levels and fluxes are missing. Stellarators are well suited to investigate the influence of such positive and negative density gradients on plasmas fluctuations and transport due to their unique capabilities to control plasma scenarios and magnetic configuration.

This paper reports on the first attempt to experimentally characterize 2-D poloidal structures of plasma profiles using the Heavy Ion Beam Probe (HIBP) diagnostic in low density ECRH plasmas in the TJ-II stellarator. The experiment has allowed the investigation of 2D poloidal contour map for plasma potential and plasma density and their fluctuations from high to low field side. In addition, the influence of positive and negative density gradients on plasma fluctuations has been investigated. Both results provide the experimental basis for future model validation of core plasma potential asymmetries and plasma stability in positive and negative gradient regions.

II. Experimental set up

TJII has a unique experimental arrangement of a dual Heavy Ion Beam Probe (HIBP) system [14]. In the experiments reported in this paper both HIBP-I and HIBP-II systems were operated in scanning and fixed point mode from the High to the Low Field Side (HFS to LFS) regions. The point of ionization or sample volume probed by the injecting beam inside the plasma in a poloidal cross-section depends on the energy of primary ion beam (Cs^+), determined by injector voltage, and on the voltages on the four set of steering plates in the primary beam line to scan the beam from HFS to LFS.

Experiments for the 2D poloidal scans were carried out in pure ECR on-axis heated regimes ($P_{ECRH} \approx 300$ kW) with constant low density in the range $n_e \sim 0.4 – 0.5 \times 10^{19}$ m^{-3} and central electron temperature in the range $T_e \sim 1$ keV. Experiments were performed for the standard magnetic configuration of TJ-II with the edge rotational transform value close to 1.6.

The plasma volume scanned by HIBP-II moves up (vertically) by 1 cm with every 2 kV increase in the injection voltage. The injector voltage was increased from 128 to 148 kV. On top of that, for each discharge and injector voltage, the sample volume is radially scanned by the beam. Hence, circa of 10 x 20 cm^2 of the plasma volume was scanned from LFS to HFS for this experiment. Measurements for local mean and relative fluctuations in plasma density and potential were obtained using parallel plate 30º proca green energy analyser in HIBP II [15]. The multi-slit analyser has 5 input slits that scans the 5 neighbouring plasma sample volumes simultaneously to measure plasma parameters mentioned before.

Fig 1 shows the estimation of the point of ionization or sample volume probed by the injected primary beam in the poloidal cross-section varying the voltage at which Cs^+ ions are injected in the range 128 – 148 kV. The primary beam is radially scanned covering HFS and LFS regions in the TJII poloidal cross section.

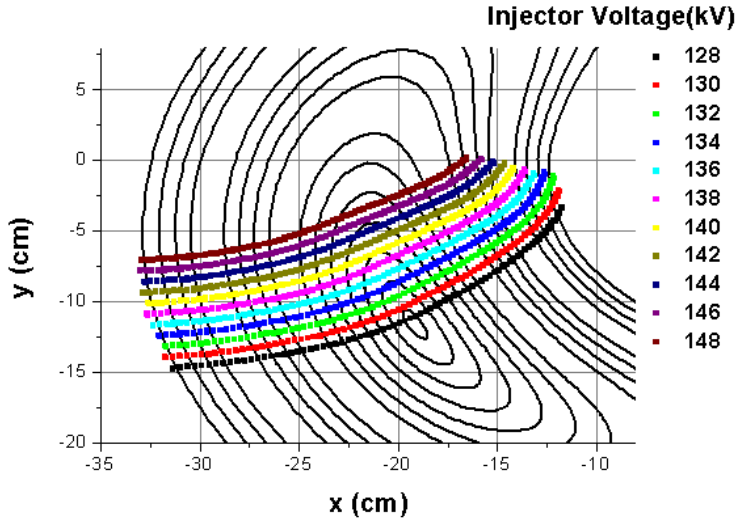

Fig1: Plasma volume scanned in TJ-II by increasing injector voltage (increasing Cs^+ energy). The point of ionization moves up and down as shown, for each injector voltage the beam was scanned from HFS to LFS for each injector voltage.

In addition, the experimental data for the investigation of the effect of positive and negative density gradient on the plasma fluctuations are also presented. The discharges were carried out for the low density ($n \approx 0.4 – 0.6 \times 10^{19}$ m^{-3}) on-axis (rho = 0) and off-axis (rho = 0.34) ECRH scenarios. These plasmas are characterized by peaked and hollow electron temperature and density profiles respectively in the TJ-II stellarator plasmas. Fig 2 shows the temperature profiles for on-axis and off-axis discharges. Temperature profile for off-axis ECR heating is flattened at the center as compared to the peaked profile at center for on-axis ECRH. The beam from HIBP-II was scanned from HFS to LFS and the power frequency spectra for fluctuations were investigated.

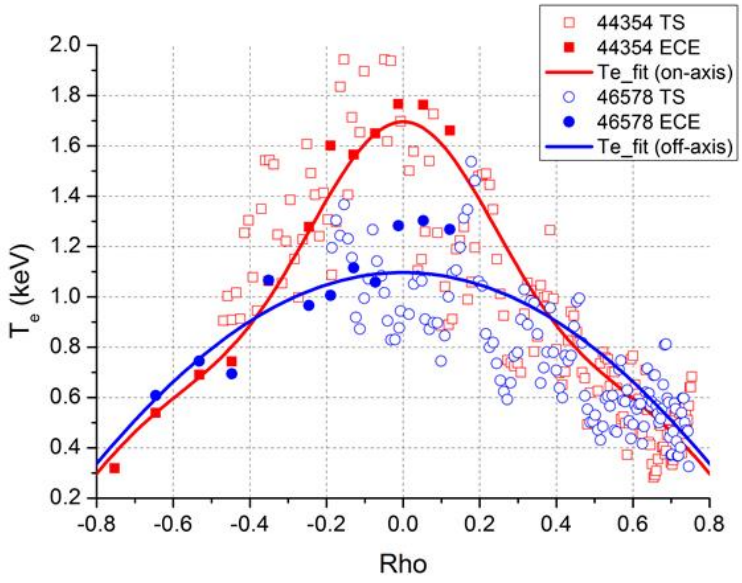

Fig 2: Electron temperature profiles for on-axis and off-axis ECRH regimes obtained by fitting the data from Thompson spectroscopy (TS) and ECE profiles.

III. Experimental results and discussion

III.1 2D Poloidal density and potential scans in ECRH on-axis experiments

The 2D analysis of averaged and root mean square (RMS) of fluctuations for plasma potential and secondary ion current is shown in Fig 3 and 4, respectively. Results are plotted over the contour plots of the vacuum magnetic flux surfaces in TJ-II.

In low density plasmas ($n \approx 0.4 \times 10^{19}$ m^{-3}) core plasma potential is positive with values in the range of +1000 V, corresponding to positive (electron root) radial electric field (E_r) in agreement with neoclassical predictions [Fig. 3]. The root mean square (rms) of potential fluctuations increases radially inwards from values in the range of 15 V in the edge to 50 V in the plasma core. Although, the contour plot for potential and rms of potential fluctuations seems rather close to the magnetic flux surfaces, some discrepancies should be noted. The 2D map for the absolute plasma potential (Fig 3, left) have a local maximum that is slightly shifted (1 – 2 cm) upwards from the axis of vacuum magnetic flux surfaces to the high field side. The local maximum of RMS fluctuations of potential (Fig 3, right) is also shifted upward. These shifts could be accounted due to uncertainties in the primary beam trajectory calculations. In addition, top – bottom and LFS - HFS poloidal variation of average potential on vacuum magnetic surfaces (in the range of 50V) have been observed (Fig 3). These values could be consistent with asymmetries of plasma potential reported by probe and Doppler measurements in ECRH electron root scenarios [16, 4]. As shown in Fig. 3 right, in the explored plasma scenarios no evidence of strong spatial localization in rms fluctuation levels in potential was observed.

The secondary ion current (I) measured by HIBP is proportional to the plasma density

for low plasma density (low attenuation), as in this experiment. Hence, normalize level of secondary ion current fluctuations, $\tilde{I}_{rms}/I$ is proportional to normalised density fluctuations, $\tilde{n}/n$ and secondary ion current (I) measurement is a proxy to the plasma density profile.

Fig 4 presents the 2D poloidal map for average (left) and normalized rms (right) values of secondary ions current (I). A local minimum in the rms of secondary current fluctuations is located at the position of local maximum of total secondary current (I) [see section III.2]. The up-down poloidal variation in total secondary current (fig4, left) could be accounted due to the instrumental effects due to the variation of Cs^+ primary current with the acceleration voltage (in the range 128 – 148 kV).

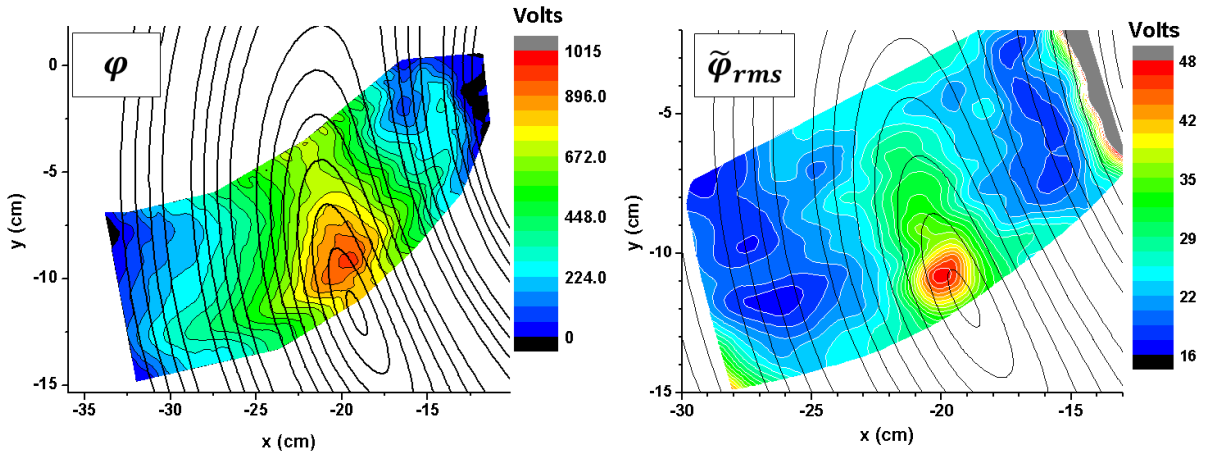

Fig 3: 2D poloidal mapping of mean potential (left) and RMS potential fluctuations (right) for the line average densities ranging between 0.43 - 0.47 ×10^{19} m^{-3}; discharges presented (from 128kV to 138, respectively): #44393, #44389, #44354, #44356, #44357, #44362, #44364, #44366, #44370, #44380, #44388.

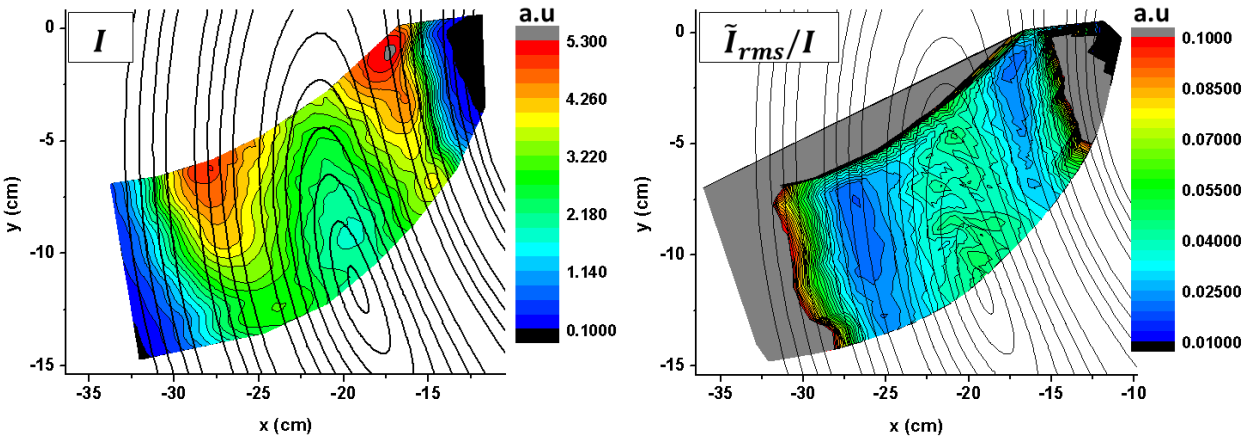

Fig 4: 2D poloidal map for average (left) and rms (right) values of secondary ion current, which is a proxy of density fluctuations.

III.2 Effect of positive and negative density gradient on fluctuations

III.2.a ECRH on-axis experiments

Fig 5 (left) presents the radial profiles of the normalized level of secondary ion current fluctuations for different injector voltages for the results obtained during the 2-D poloidal scan [see Fig. 4]. A local minimum in the normalized fluctuation levels ($\tilde{I}_{rms}/I$) appears both in the HFS and LFS at rho ~ 0.6. This minimum appears for all acceleration voltages (i.e. at different poloidal locations), illustrating the reproducibility of experimental results. The radial location of these minima is correlated with the peaks (maximum) of the secondary ion current (I) profile, i.e. the transition from positive radial gradients in density profiles (fig 5, right). The fig 5, right shows the rms fluctuation in relative density and secondary ion current for a single scan (injector voltage = 132 kV) from HFS to LFS along with the ECRH hollow secondary ion current profile.

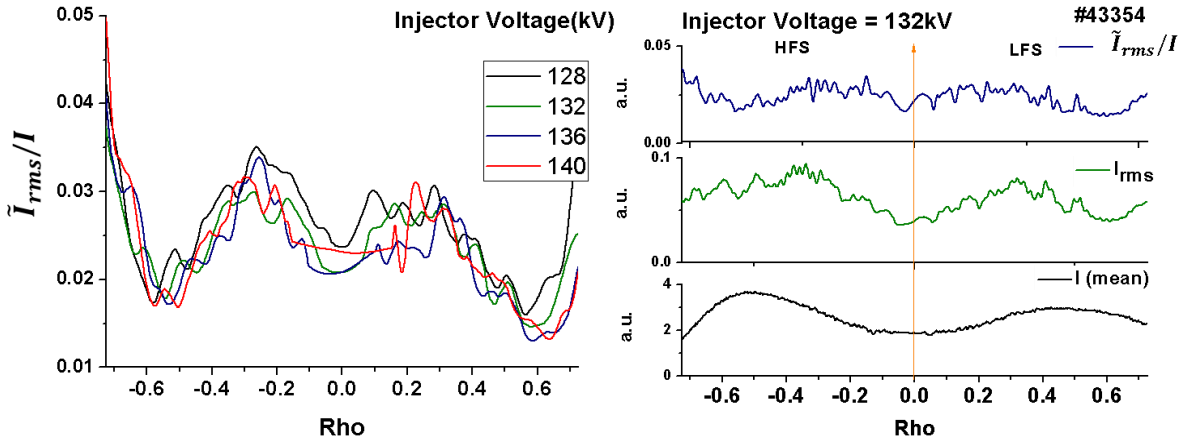

Fig 5: Profiles of normalized rms current fluctuation level for 4 injector voltages (left); radial profiles for rms fluctuation levels in I and I normalized ($\tilde{I}_{rms}/I$) value in hollow ECRH density profile for injector voltage of 132kV. A local minima is observed in I relative fluctuations at the peaks of the I profile (right).

The frequency spectra of density fluctuations along with the radial secondary ion current (I) profile for on-axis (rho = 0) ECR heated plasma is presented in figure 6 and the same is plotted with respect to Rho in figure 7. The secondary ion current profile for on-axis ECRH indicates more peaked value in the HFS at the transition from negative to positive gradient regions (Rho ≈ -0.5). The normalized level of density fluctuations ($\tilde{I}_{rms}/I$) is much larger in the negative (Rho = 0.7 – 1) than in the positive (Rho = 0.5 – 0.3) density gradient region, with a minimum in the proximity of the zero density gradient region (Rho ≈ 0.6). The level of density fluctuations in both positive and

negative density regions are dominated by broadband frequencies (<100 kHz as shown in fig. 6 and 7) with the positive gradient region exhibiting quasi-coherent modes.

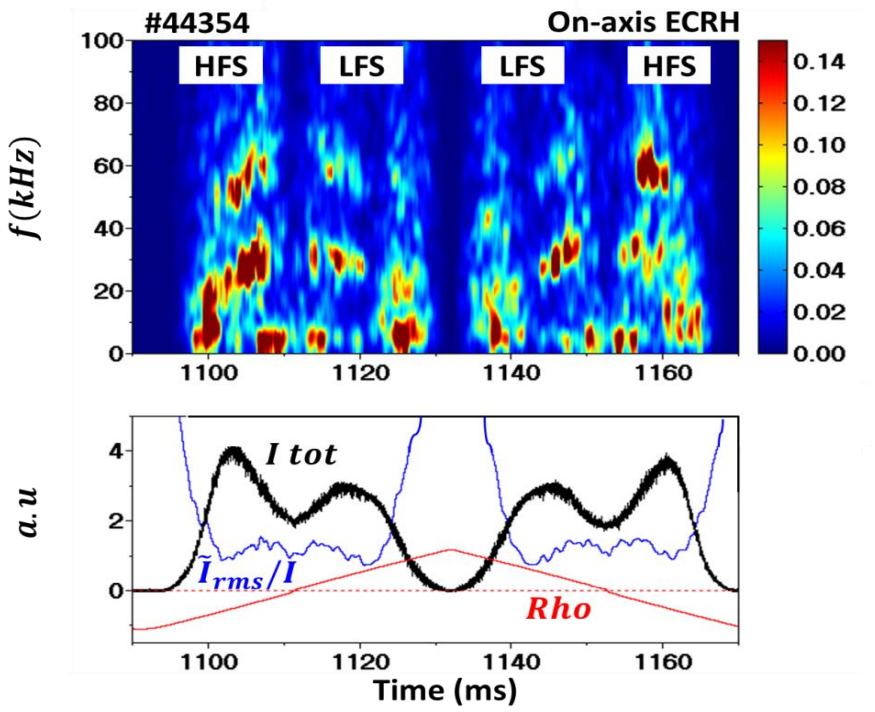

Fig 6*: Radial profile of density fluctuations measured during the time scan of the HIBP system in the TJ-II stellarator (ECR on-axis heating) for 2 consecutive radial scans*

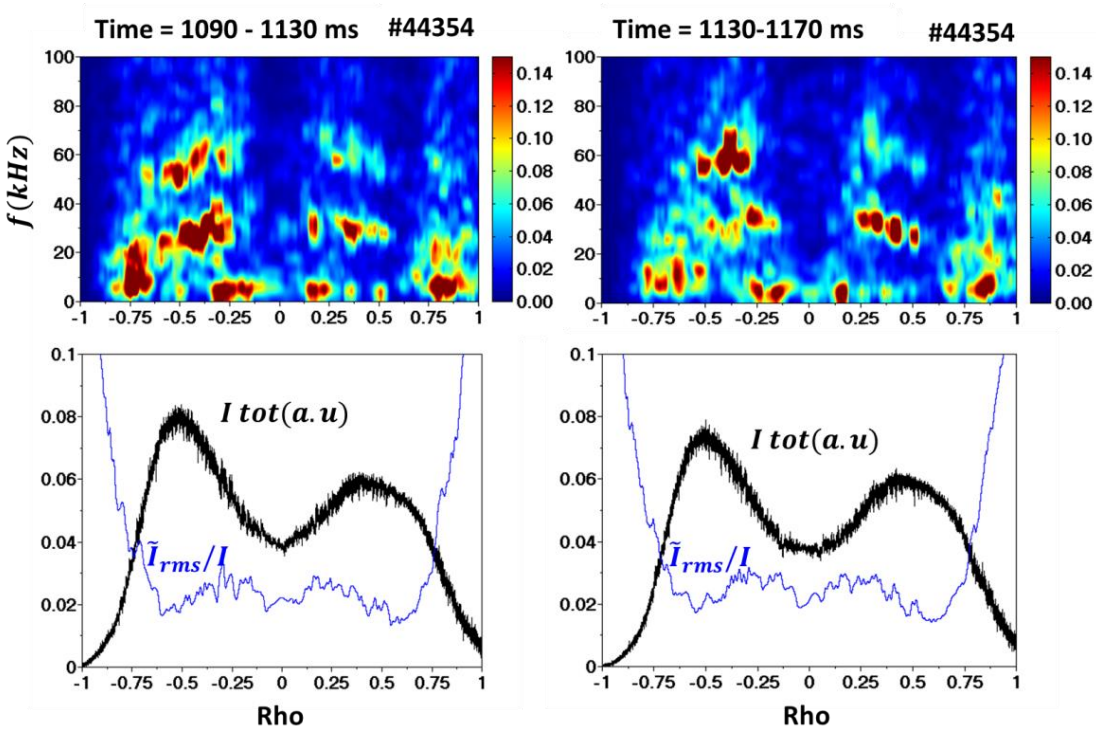

Fig 7: *Spectral frequency fluctuations in the secondary ion current with respect to rho along with the secondary ion profile measured by HIBPII for on-axis (rho = 0) ECR heated plasma for 2 radial scans.*

III.2.b ECRH off-axis experiments

Figure 8 and 9 display the mean secondary ion current (I), normalized level of density fluctuations and spectral frequency fluctuations in the secondary ion current measured by HIBPII for off–axis (rho = 0.34) ECRH heated plasmas. The spectral frequency distribution for the two scans presented in fig 8 is plotted with respect to the rho value in fig 9. Fluctuations in the secondary ion current appear both at the positive and negative gradient regions, with the relative amplitude of density fluctuations higher in the negative gradient region [Fig. 8 and 9]. Fluctuations are dominated by broadband frequencies (<100 kHz as shown in fig. 8) in the negative density gradient region and eventually by quasi-coherent modes in the positive gradient region [off-axis ECRH scenarios]. Furthermore, plasma frequency fluctuations are poloidally asymmetric, showing broader frequency spectra in the LFS than in the HFS (Fig 9). Therefore, experimental results in off-axis ECRH scenarios shows a clear influence of positive & negative density gradient regions on plasma fluctuations with most unstable modes located in the negative density gradient region.

Finally, it should also be noted that secondary ion current (I) profiles have higher peaked amplitude at the transition from positive to negative gradient regions in LFS for off axis ECRH plasma (see fig 8), unlike the on-axis ECRH profile (see fig 7). The origin of these plasma density asymmetries and its dependence with TJ-II plasma scenarios is under investigation.

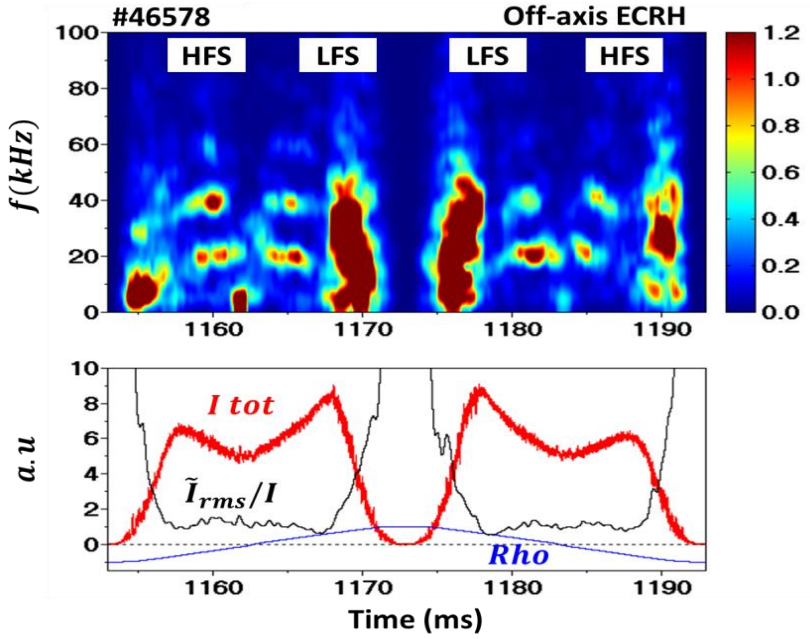

Fig. 8 Radial profile of density fluctuations measured during the time scan of the HIBP system in the TJ-II stellarator (ECR off-axis heating)

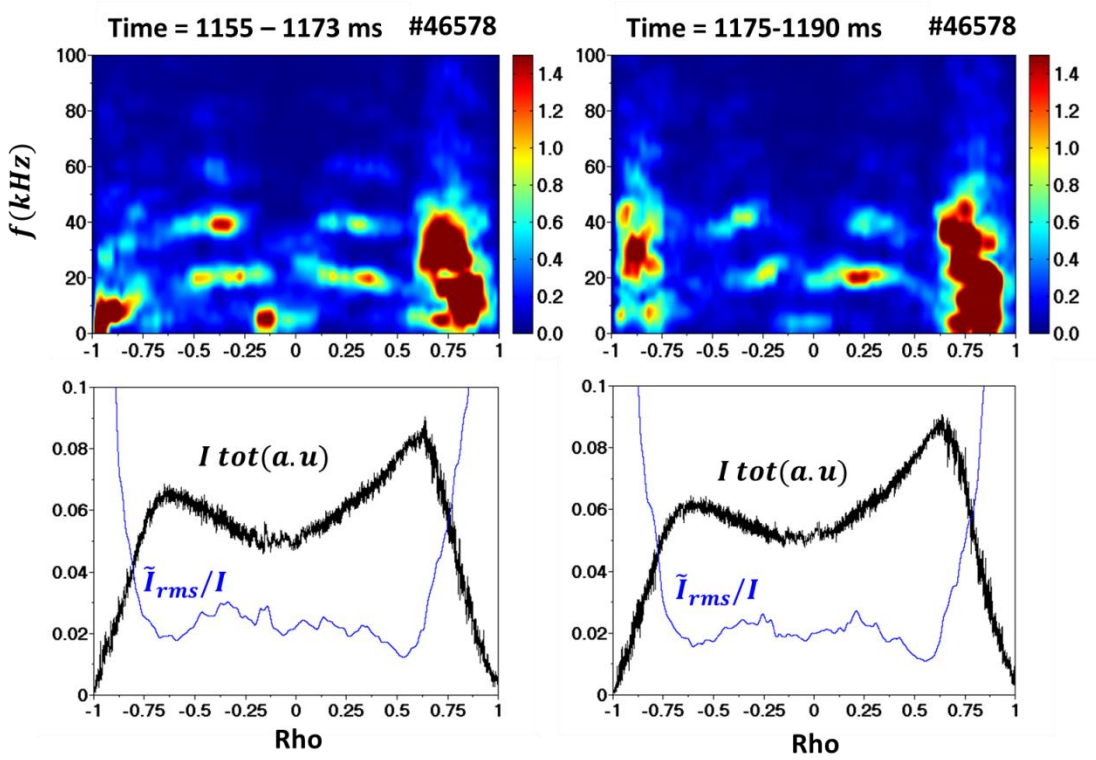

Fig 9: Spectral frequency fluctuations in the secondary ion current with respect to rho along with the secondary ion profile measured by HIBPII for off-axis (rho =0.34) ECRH plasmas

IV. Conclusions

For the first time 2D poloidal contour plots of plasma potential and density and their fluctuations have been measured in low density plasmas with hollow density profiles sustained by ECRH in the TJ-II stellarator with the following conclusions:

a) The 2D map for the absolute plasma potential have a local maximum in the plasma core as expected in electron root scenarios. The 2D mapping of plasma potential shows a mismatch with vacuum magnetic calculations that could be partially explained by instrumental effects.

b) Density fluctuations appear both at the positive and negative gradient regions for ECRH plasmas. Normalized levels of density fluctuations are stronger in the negative density gradient than in the positive gradient region. Frequency spectra are dominated by frequencies below 100 kHz with different spectral characteristics in the positive and negative gradient regions that are affected by the ECRH scenario (on vs off-axis heating).

The TJ-II innovative experimental set-up, developed using a dual HIBP diagnostic, paves the way to validate models on core plasma potential asymmetries and particle fuelling under positive density gradient scenarios in the TJ-II stellarator.

On-going experiments are in progress to quantify systematically the influence of the shape of temperature and density profiles on the level of fluctuations and transport in the positive & negative gradient regions. Future work will include new experiments in order to expand the 2D mapping towards the whole TJ-II poloidal cross section.

The work of Kurchatov team was funded by Russian Science Foundation, project 14-22-00193. The work of AVM was partly supported by the Competitiveness Program of NRNU MEPhI. The work of Kharkov team was funded by STCU, project P-507F. IPFN activities received financial support from "Fundação para a Ciência e Tecnologia" through project UID/FIS/50010/2013. R. Sharma is supported by the Fusion DC Erasmus programme. This work has been carried out within the framework of the EUROfusion Consortium and has received funding from the Euratom research and training programme 2014-2018 under grant agreement No 633053. The views and opinions expressed herein do not necessarily reflect those of the European Commission.

References

[1] C. Hidalgo et al., Plasma Phys. Control. Fusion *37* (1995) A53

[2] C. Hidalgo et al., Plasma Phys. Control. Fusion 59 (2017) 014051

[3] P. Xanthopoulos et al., Physical Review X 6 (2016) 021033

[4] E. Sánchez et al. 2018 Validation of global gyrokinetic simulations in stellarator configurations 27th IAEA Fusion Energy Conference (FEC 2018) EX/P1-11; T. Estrada et al. 2018 Turbulence and radial electric field asymmetries measured at TJ-II plasmas 27th IAEA Fusion Energy Conference (FEC 2018) EX/P1-9

[5] Z.Yan et al., PRL 112 (2014) 125002

[6] S J Zweben et al., Plasma Phys. Control. Fusion 49 (2007) S1

[7] A. Shimizu et al., Review of Scientific Instruments 87 (2016) 11E731

[8] M. Valovic et al Nucl. Fusion 48 (2008) 075006

[9] P. Vincenzi et al., Nuclear Fusion 55 (2015) 113028

[10] A. Dinklage et al., Nucl. Fusion 57 (2017) 066016

[11] L. Garzotti et al Plasma Phys. Control. Fusion 56 (2014) 035004

[12] C. Angioni et al., Nucl. Fusion 57 (2017) 116053

[13] D. Tegnered et al., Journal of Physics: Conference Series 775 (2016) 012014

[14] A.V. Melnikov *et al.* Nucl. Fusion 57 (2017) 072004

[15] A.V. Melnikov et al., Fusion Eng. Des (2015)

[16] M. A. Pedrosa et al., Nuclear Fusion 55 (2015) 052001.